RSC Advances

ROYAL SOCIETY OF CHEMISTRY

www.rsc.org/advances

RSC Advances

PAPER

Effects of Furan Ring in Epoxy Resin on Thermomechanical Properties of Highly Cross-linked Epoxy Networks: A Molecular Simulation Study

Received 00th January 2015,
Accepted 00th January 20xx

DOI: 10.1039/x0xx00000x

www.rsc.org/

Kai Li,[a] Ni Huo,[a] Xinping Liu,[a] Jue Cheng*[a] and Junying Zhang*[a]

Two highly cross-linked epoxy networks based on two epoxy resins model compounds with similar structures, 2,5-bis[(2-oxiranylmethoxy)-methyl]-furan (BOF) and 2,5-bis[(2-oxiranylmethoxy)methyl]-benzene (BOB), and the same curing agent PACM were constructed by using molecular dynamic simulations. Several thermomechanical properties of these two systems including glass transition temperatures, coefficients of thermal expansion, Young's moduli, and Poisson's ratios were calculated. The simulated values were compared with the available experimental results, and good agreements were obtained. This consistency proved the validity of the atomistic models. The changes of aromatic structures in the epoxy monomers from phenyl to furyl lead to higher glassy Young's modulus of the cross-linked epoxy network. This phenomenon can be illustrated by the reduced mobility of the polymer chains arising from the increased packing efficiency. These changes are considered to be induced by the higher van der Waals energy within furan-based epoxy.

Introduction

Epoxy resins are the oligomers containing two or more epoxy groups in a single molecule. They are widely used as microelectronic packing materials, adhesives, coatings, and composites because of their numerous excellent performances including good adhesion, heat resistance, chemical resistance, and excellent mechanical and electrical performance after the reaction with proper curing agents. In general, these superior performances are derived from the generated three-dimensional networks.

The ultimate structures of the generated networks depend mainly on the detailed structures of the epoxy resins oligomers and the curing agents, conversion degree, curing conditions, and thermal history. Theoretically, by controlling these factors we can get the specific network architecture, and hence the desired performances. However, difficulties still exist in building structure–property relationships due to the complexity and infusible and insoluble nature of the networks. For example, when epoxy resins are used as adhesives or composites matrix, the internal stress generated at the interface between the epoxy resin and the substrate may cause deformation, cracking, and adhesion reduction of the interface.[1-4] According to an expression in ref [5], the Young's modulus in glassy region is one of the main factors affecting the internal stress. In other words, accurately predicting the glassy Young's modulus of the cured epoxy resin is crucial for its ultimate application.[3] However, currently there exist two controversial opinions on the relationship of glassy Young's modulus and the conversion of curing degree. One is that glassy Young's modulus is considered to rise with the increase of conversion, i.e. cross-link density. The other is that glassy Young's modulus is observed to experience a maximum with respect to the conversion.[6-10] In short, the understanding of the mechanism that affecting glassy Young's modulus of the cross-linked epoxy network is still limited though it is of great importance for the application of epoxy resins.

Compared with traditional experimental methods, molecular dynamics (MD) simulations provide an alternative method to study the structure and the properties of polymers. In comparison with studying the thermoplastics, one of the main difficulties in studying the thermosets lies in constructing the cross-linked networks accurately and efficiently. During the past few years, methodology of constructing molecular structure model of the cross-linked epoxy systems by using MD simulations has achieved progress to some degree. (1) Yarovsky et al.[11] developed a static method to construct epoxy networks with low molecular weight, where the cross-linking bonds were created simultaneously based on a predefined radius. (2) Wu and Xu[12] modeled a cross-linked epoxy system by using a dynamic cross-linking approach—carrying out energy minimization (MM) and molecular dynamics after each cross-linking reaction with a fixed cut-off reaction radius. (3) Varshey et al.[13] simulated the cross-linking reaction in a stepwise manner through steadily increasing the cut-off reaction radius followed by MD/MM simulations and proved that the stepwise cross-linking method is efficient and accurate in establishing the cross-linked networks.

[a] Key Laboratory of Carbon Fiber and Functional Polymers, Ministry of Education, Beijing University of Chemical Technology, Beijing 100029, P. R. China
E-mail: zhangjy@mail.buct.edu.cn; chengjue@mail.buct.edu.cn; Fax: (86) 010-64426439; Tel: (86) 010-64425439.

Using the methods described above, several research works[14-21] on the structure–property relationships of the cross-linked epoxy networks have been reported, which mainly focused on the effects of external factors including cooling rate, temperature, and strain rate on the thermomechanical properties of cross-linked epoxy systems. However, relatively few works investigate the effects of chemical structures of epoxy resins and cross-linkers. Soni et al.[17] used MD simulations to study the effects of the cross-linker length and flexibility on the properties (density, coefficient of volume thermal expansion, and T_g) of the cross-linked systems formed by diglycidyl ether of bisphenol A (DGEBA) and four poly(oxypropylene) (POP) diamines with different lengths ranging from 3 to 68 units of oxypropylene. Yang et al.[20] investigated two similar cross-linked epoxy systems based on epoxy TDE85, cured with 2,2′-bis(trifluoromethyl)-4,4′-diamino biphenyl (TFMB) and 2,2′-dimethyl-4,4′-diaminobiphenyl (MTB) respectively, to establish the structure–property relationships via both experiment and molecular simulation. They studied the effects of amine structures on the T_g by analyzing the conformation and the cohesive energy density (CED) of each system. Their results showed that TFMB is stiffer than MTB and the CED of TFMB–TDE85 is higher than that of MTB–TDE85, and they concluded these are the reasons why the T_g of the TFMB–TDE85 is higher. Sirk et al.[22] studied the effects of flexibility of the cross-linker on the thermomechanical properties of the cross-linked epoxy networks which were constructed based on DGEBA and curing agent mixtures composed of a flexible cross-linker POP and a stiff cross-linker 4,4'-methylenebis(cyclohexylamine) (MCA) by using MD simulations. They specially interpreted the weaker and broader glass transition appearing in the relatively stiff systems, i.e. cross-linked epoxy networks formed with more MCAs in the curing agent mixtures.

The studies above proved molecular simulations an effective method of investigating the structure–property relationships of the cross-linked networks. However, to our best knowledge, no simulation works have ever focused on the effects of monomer structures on glassy Young's modulus of the ultimate cross-linked networks.

In this work, two highly cross-linked epoxy networks were constructed by molecular simulations via a stepwise cross-linking method. They are of similar structures except for the variation of the aromatic rings (one is benzene ring, while the other is furan ring). Validity of the model structures was proved by comparing a number of thermomechanical properties obtained in our molecular simulations with available experimental or simulated ones. Special emphases were put on exploring the effects of the detailed chemical structures on the glassy Young's modulus. This work provides a general method of predicting the thermomechanical properties of cross-linked epoxy networks, as well as, studying the effects of detailed chemical structures on the properties. It is expected to provide guidance to designing the cross-linked epoxy networks with specific thermomechanical properties.

Simulation Details

Forcefields

Polymer Consistent Force-Field (PCFF),[23,24] one of the second-generation forcefields, proved to be an effective forcefield to predict the thermomechanical properties of the organics.[11,19,25,26] In all our molecular mechanics and MD simulations, PCFF is used to describe the interactions between particles in the systems. The functional forms of the energy terms used by PCFF are given as follows:

$$\begin{aligned}
E_{pot} &= \sum_b \left[k_2(b-b_0)^2 + k_3(b-b_0)^3 + k_4(b-b_0)^4\right] \\
&+ \sum_\theta \left[H_2(\theta-\theta_0)^2 + H_3(\theta-\theta_0)^3 + H_4(\theta-\theta_0)^4\right] \\
&+ \sum_\varphi \left[V_1(1-\cos\varphi) + V_2(1-\cos 2\varphi) + V_3(1-\cos 3\varphi)\right] + \sum_\chi K_\chi \chi^2 \\
&+ \sum_{b,b'} F_{bb}(b-b_0)(b'-b'_0) + \sum_{b,\theta} F_{b\theta}(b-b_0)(\theta-\theta_0) + \sum_{\theta,\theta'} F_{\theta\theta'}(\theta-\theta')(\theta-\theta') \\
&+ \sum_{b,\varphi} (b-b_0)(V\cos\varphi + V_2\cos 2\varphi + V_3\cos 3\varphi) \\
&+ \sum_{\theta,\varphi} (\theta-\theta_0)(V\cos\varphi + V_2\cos 2\varphi + V_3\cos 3\varphi) \\
&+ \sum_{b,\theta,\varphi} F_{b\theta\varphi}(b-b_0)(\theta-\theta_0)\cos\varphi \\
&+ \sum_{i,j} \frac{q_i q_j}{\varepsilon r_{ij}} + \sum_{i,j}\left[\frac{A_{ij}}{r_{ij}^9} - \frac{B_{ij}}{r_{ij}^6}\right]
\end{aligned} \quad (1)$$

The total energy is written into valence, crossterm, and nonbond interactions, as is seen from Eq. (1). The valence terms comprise of bond stretching, angle bending, dihedral angle torsion, and inversion (also called out-of-plane) interactions, and the crossterm are the coupling between them. The nonbond terms comprise of the electrostatic and van der Waals (vdW) interactions. The subscripts *i* and *j* represent pairs of atoms that are interacted. The vdW interactions are obtained from Lennard–Jones (LJ) 9–6 function. For the MD simulations performed in all of this work, the vdW interactions were calculated with a cutoff distance of 12.5 Å, while the electrostatic interactions were calculated using the Ewald summation with an accuracy of 1×10^{-5}.

Model Systems and Cross-linking Process

The cross-linked epoxy systems studied in this work were based on two similar epoxy monomers with different aromatic rings, 2,5-bis[(2-oxiranylmethoxy)-methyl]-furan (BOF) and 2,5-bis[(2-oxiranylmethoxy)methyl]-benzene (BOB), and the same cross-linker 4,4′-diaminodicyclohexylmethane (PACM). Their chemical structures are illustrated in Figure 1. The mechanism of the cross-linking reaction is illustrated in Figure 2. A stoichiometric mixture of 400 epoxy monomers (BOB/BOF) and 200 cross-linkers (PACM) was placed in a cubic simulation cell using the Amorphous Cell module in the Material Studio software[27] with the initial density of 1.1 g/cm^3, which is the typical value for uncross-linked epoxy systems. Relatively large models were constructed to make sure the isotropy of the final cross-linked systems. Then the monomers were randomly seeded within the simulation cell following the self-avoiding random walk method of Theodorou and Suter.[28,29] Periodic boundary conditions were employed in all directions for all

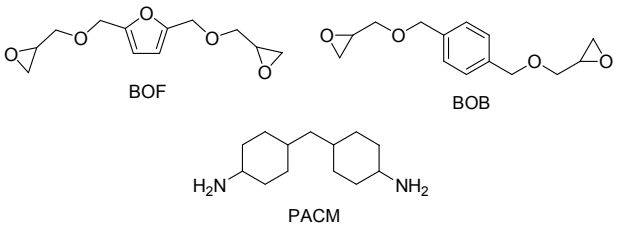

Figure 1. Chemical structures of epoxy monomers (BOB and BOF) and cross-linker (PACM).

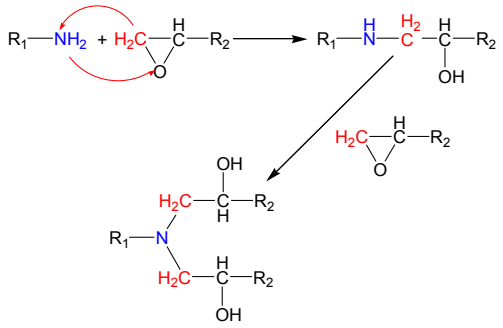

Figure 2. Schematic illustration of the curing reaction mechanism of the epoxy–amine polymerization.

simulations in order to eliminate the surface effects of the models.

The initial uncross-linked systems were equilibrated for 200 ps in the isothermal and isochoric ensemble (NVT) at 300 K, followed by another 1 ns equilibration in the isothermal and isobaric ensemble (NPT) in atmospheric pressure at 300K. The Nose–Hoover thermostat and Berendsen barostat were used for temperature and pressure control, respectively. The corresponding integration time step was 1 fs. Once the systems were equilibrated, the cross-linking procedure was performed as follows.

Figure 3 shows the flowchart illustrating the cross-linking procedure for both of the cross-linked systems. Both of the two cross-linked epoxy systems, BOB–PACM and BOF–PACM, were constructed based on the same procedure as follows: First, new bonds were repeatedly created between all the reactive pairs (epoxy carbon and amine nitrogen) within a predefined cutoff distance. In order to accelerate the cross-linking progress and facilitate the relaxation of the newly generated topology, the cutoff distance gradually increased. In this work, it was initially set to be 4 Å and increased to 11 Å with an increment of 1 Å. Then a progress of MM and 50 ps NPT MD simulations was performed to relax the system and make the reactive atoms close to each other. For each increment of the cutoff distance, this progress repeated five times unless no reactive pairs within the cutoff distance was found. The cross-linking process ends if the predetermined conversion limit or maximum cutoff distance is reached. At last, if the final conversion degree exceeds the limit, the created

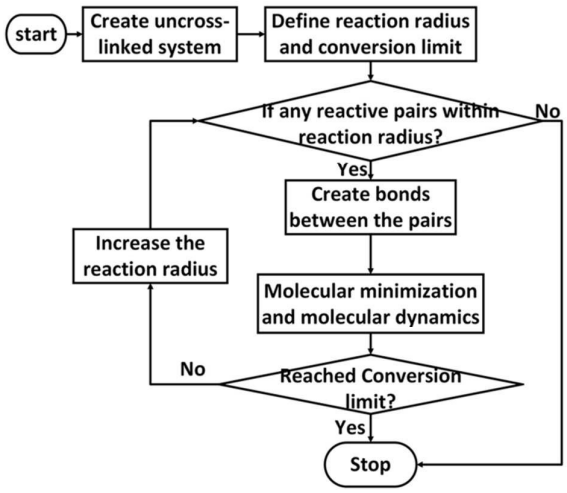

Figure 3. Flowchart of cross-linking procedure used in the construction of epoxy networks.

bonds should be randomly broken back into the epoxy ring and amino to make sure the conversion degree is the conversion limit exactly. The conversion limit in this work was set to be 90%. It was reached when the cutoff distance is 10 Å for both of the systems. It should be mentioned here that although many experimental works claim that their conversion is 100% measured by using experimental techniques including Fourier transform infrared spectroscopy (FTIR) and differential scanning calorimetry (DSC), it does not mean that all of the reactive sites are cross-linked. Meanwhile, several simulation works[13,30,31] have shown that by setting the conversion in the range of 85% to 95%, the predicted results agree well with the experimental ones.

Given the significant role they play in the electrostatic interactions, the partial charges should be updated immediately with changes of the chemical environment around the reactive atoms during the cross-linking progress. This was accomplished by using the bond increment charging algorithm[24,32] of the PCFF. In the algorithm, the charge q_i for atom *i* is calculated as a summation of every related charge bond increment, δ_{ij}, which represents partial charge between atom *i* and atom *j*:

$$q_i = \sum_j \delta_{ij} \quad (2)$$

where *j* runs over all the atoms which are bonded to atom *i* directly.

In the end, the cross-linked system was equilibrated by combining the MD and MM simulations to obtain fully relaxed network for the following analysis. The MD simulations consist of following steps: first the NVT equilibration at 600 K for 1ns; then NVT annealing to 200 K at the cooling rate of 10 K/20 ps; last NPT equilibration at 200 K and atmospheric pressure for 2 ns.

The final structures of the two cross-linked epoxy systems were shown in Figure 4. The density at room temperature is 1.07 and 1.10 g/cm^3 for BOB–PACM and BOF–PACM system,

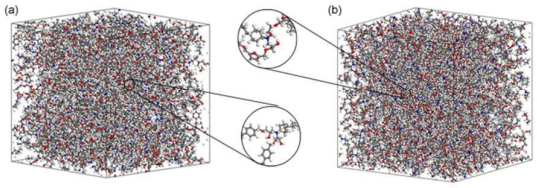

Figure 4. Molecular structures of the two cross-linked epoxy systems: (a) BOB–PACM and (b) BOF–PACM.

respectively. For further mechanical analysis, the fully relaxed model systems were converted into the input data of LAMMPS.[33]

Results and Discussion

Glass Transition Temperature

The well-relaxed network of each cross-linked epoxy system obtained above experienced an equilibration at 600 K in NPT, followed by an annealing simulation, i.e. a slowly cooling down process at the rate of 10 K/50 ps to 200 K using NPT MD simulations. According to the results from the annealing simulation, the dependence of density on the temperature for each cross-linked system was shown in Figure 5. From the curve of each structure, we can see that there is a characteristic turning point in the slope of the density–temperature curve, where the temperature is corresponding to T_g. To obtain the exact value of T_g, linear fit with 95% confidence was performed to the temperature-density data. The predicted and the experimental T_gs for the two cross-linked systems were listed in Table 1. The predicted T_gs for the two cross-linked systems are both about 30 K higher than those obtained from experiments. These T_g shifts can be explained by using the Williams–Landel–Ferry (WLF) equation.[34] Given that the cooling rates in the simulation are 10 orders higher than those employed in the experiments, the T_g shifts are considered reasonable.

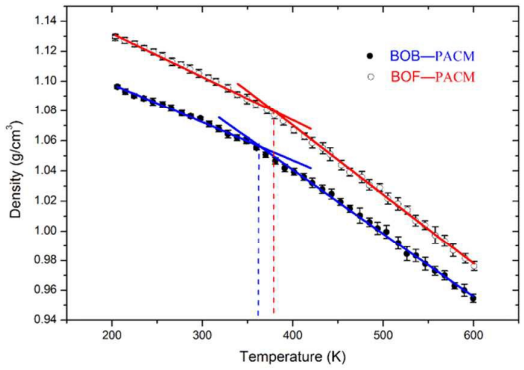

Figure 5. The temperature dependence of density of BOB–PACM and BOF–PACM.

Table 1. The calculated glass transition temperatures of BOB–PACM and BOF–PACM systems and their experimental values

System	Glassy transition temperature (K)	
	Simulation	Experiment
BOB–PACM	363.88	336.15 (ref. 37)
BOF–PACM	379.87	353.15 (ref. 37)

Coefficients of Thermal Expansion

The coefficient of volume thermal expansion (CVTE), α, is calculated using the following equation:

$$\alpha = \frac{1}{V_0}\left(\frac{\partial V}{\partial T}\right)_P \quad (3)$$

where V is the volume of the cross-linked system at temperature T, V_0 is the volume of the simulation cell at 200 K, and the subscript P represents a constant-pressure process. For the cured epoxy system, an isotropic material, the coefficient of linear thermal expansion (CLTE), β, is related to α as

$$\beta = \frac{1}{L_0}\left(\frac{\partial L}{\partial T}\right)_P = \frac{\alpha}{3} \quad (4)$$

The fractional volume change (V-V_0/V) as a function of temperature for each cross-linked system was plotted in Figure 6. Linear fits were performed on the curves in both regions below and above T_g, and the CVTEs were obtained from the slops of the linear regression lines. The CLTE results calculated using the Eq. (4) were shown in Table 2. The corresponding CLTE in the glassy and rubbery region of the two systems are both in the ranges of typical cross-linked epoxy systems obtained by experimental and simulation studies (40–100 ppm/°C in glassy region and 100–200 ppm/°C in rubbery region).[13,17,35,36]

Uniaxial Tension

Tensile deformation for each of the system was performed at 200 K via non-equilibrium MD simulations with the cell length along the loading direction continuously elongated, while maintaining atmospheric pressure in the transverse directions. The low temperature was selected to eliminate the effects of the different T_gs of the two systems on the mechanical properties. The simulation cell in the directions perpendicular to the tensile axis would shrink automatically according to the Poisson's effect. Periodical boundary condition was applied. The rate of deformation applied in MD simulation of tensile test was 1×10^8 s^{-1}, a typical rate in MD simulations, which is much higher than those applied in experimental tensile tests due to the limitations of total simulation time. However, previous studies have shown that the calculated Young's modulus in polymeric materials using MD simulations is not sensitive to the change of strain rate.[16,19] During the tensile progress, the stress components both in the tensile and

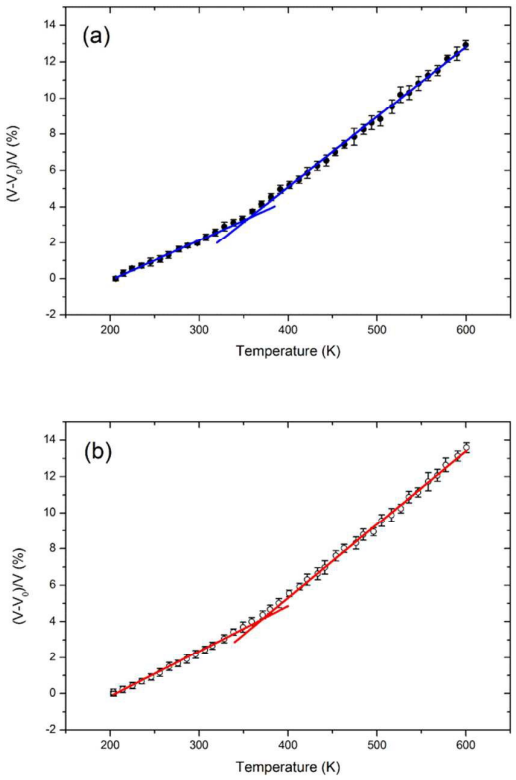

Figure 6. The fractional change in volume $(V\text{-}V_0)/V$ as a function of temperature for (a) BOB–PACM and (b) BOF–PACM.

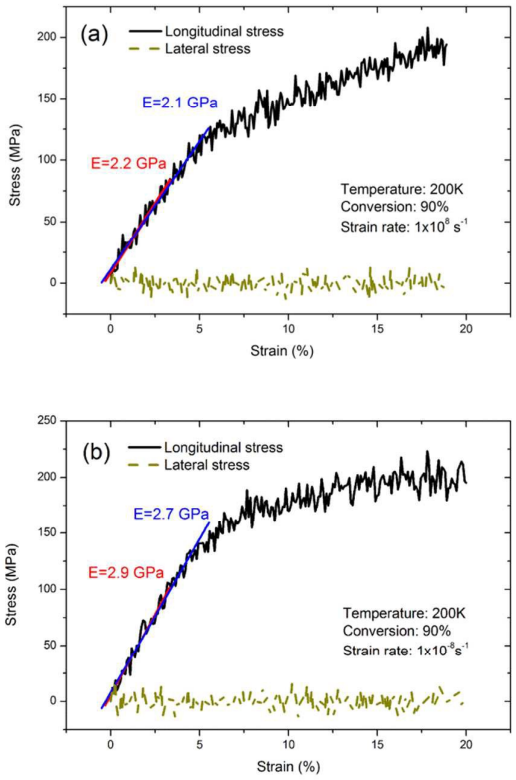

Figure 7. Stress vs. strain curves of (a) BOB–PACM and (b) BOF–PACM.

transverse directions as well as the lateral shrinkage of the cell were recorded in each step. The stresses as a function of the strain were plotted in Figure 7, and the lateral strain as a function of the longitudinal strain was plotted in Figure 8. Similar to the previous results reported,[15,16,19] the MD simulations did not show the brittle nature of the highly cross-linked epoxy. This phenomenon may be attributed to the small system size, in other words, the simulated deformation is extremely localized.

The Young's modulus for each of the cross-linked system was obtained by performing a linear regression analysis of the longitudinal stress versus strain data up to strains within the linear response region of the system and calculating its slope. By fitting the MD data to the strain range of [0, 3%] and [0, 5%], the calculated Young's modulus is within the range of 2.1–2.2 and 2.7–2.9 GPa for the BOB–PACM and BOF–PACM systems, respectively. The MD predictions are consistent with the experimental values (about 2.2 GPa and 2.8 GPa for BOB–

Table 2. The calculated values of density and CLTE of the BOB–PACM and BOF–PACM systems

System	Density (g/cm^3)	CLTE–glassy (ppm)	CLTE–rubbery (ppm)
BOB–PACM	1.07	74.3	129
BOF–PACM	1.12	83.4	135

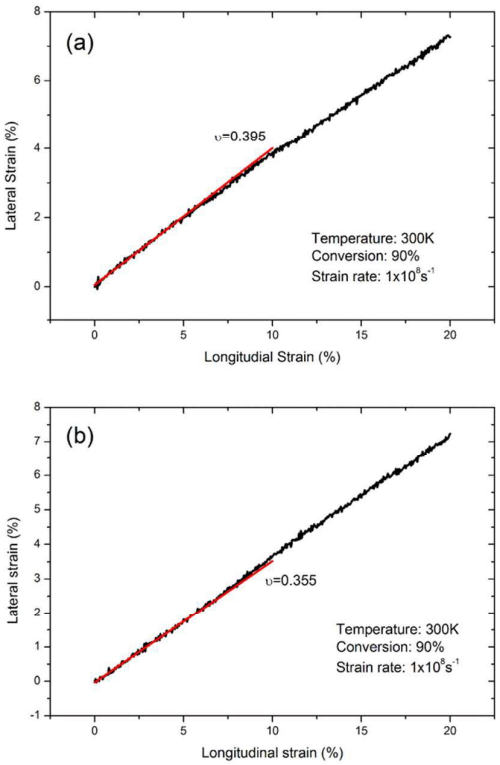

Figure 8. The lateral strain vs. longitudinal strain of (a) BOB–PACM and (b) BOF–PACM.

PACM system and BOF–PACM system, respectively) obtained from the DMA data in ref [37]. In general, the glassy Young's modulus of the BOF–PACM system is higher than that of the BOB–PACM system, that is, BOF contributes to the improvement of the mechanical properties of the cross-linked epoxy system. The Poisson's ratios of the BOB–PACM and BOF–PACM systems obtained by performing linear regression are 0.40 and 0.36 respectively, which are both in the range of 0.30–0.46 for typical cross-linked epoxy networks.

Microscopic Structure and Hydrogen Bonds

The microscopic details of the systems were analyzed by calculating the radial distribution functions (RDFs). The RDF describes the probability of atoms β appear in the distance *r* away from atoms α:

$$g_{\alpha\beta}(r) = \frac{V}{n_\beta} \frac{n_\beta(r)}{4\pi r^2 \Delta r} \quad (5)$$

where n_β is the numbers of atoms studied, *V* is the cell volume, and $n_\beta(r)$ is the number of β atoms within the range of (r, $r + \Delta r$) corresponding to α atoms. Figure 9 shows the RDFs of all the atoms for the two cross-linked epoxy systems at temperature 200K. The two systems share common features due to their similar structures. No RDF appears within short distance less than 0.9 Å because of the excluded volume effects. The first peak around 0.97 Å is attributed to the bond length of hydroxyl created during the cross-linking reaction, where the peak of the BOF–PACM is slightly stronger due to its relatively higher density. The second and largest peak around 1.11 Å is attributed to bond length between hydrogen and carbon or nitrogen. The third peak around 1.41 Å is attributed to bond length of the aromatic ring, where peak of the BOB–PACM system is relatively strong because the number of bonds in benzene ring is one more than that in furan ring. The forth peak around 1.55 Å is attributed to the bond length of the carbon and non-hydrogen atoms. The peaks at the distance larger than 1.55 Å is attributed to the distances between atoms one or more bonds apart. The RDFs converge to 1 at large distances proving the amorphous and isotropy nature of the cross-linked system.

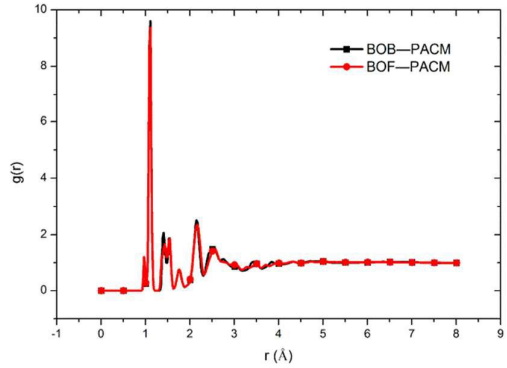

Figure 9. The radial distribution functions (RDFs) for all the atoms in the cured epoxy systems.

The epoxy systems cured by amine contain many newly generated hydroxyls, so they tend to produce large amounts of hydrogen bonds, which significantly increase the intermolecular interaction and may consequently affect the mechanical properties of the cross-linked epoxy. As the forcefield PCFF is used, the H–bonds implicit in the nonbond interaction term, thus we specially studied the RDFs between the atoms pairs that form most H–bonds. The atom pairs that most possibly form H–bonds are composed of hydroxyl–hydroxyl, hydroxyl–ether, and hydroxyl–amine. The corresponding RDFs were plotted in Figure 10, which reveal the sharp peaks at about 2.8 Å associated with regular H–bonds and at about 3.60 Å associated with twist H–bonds. No clear distinctions were found between the two systems, which

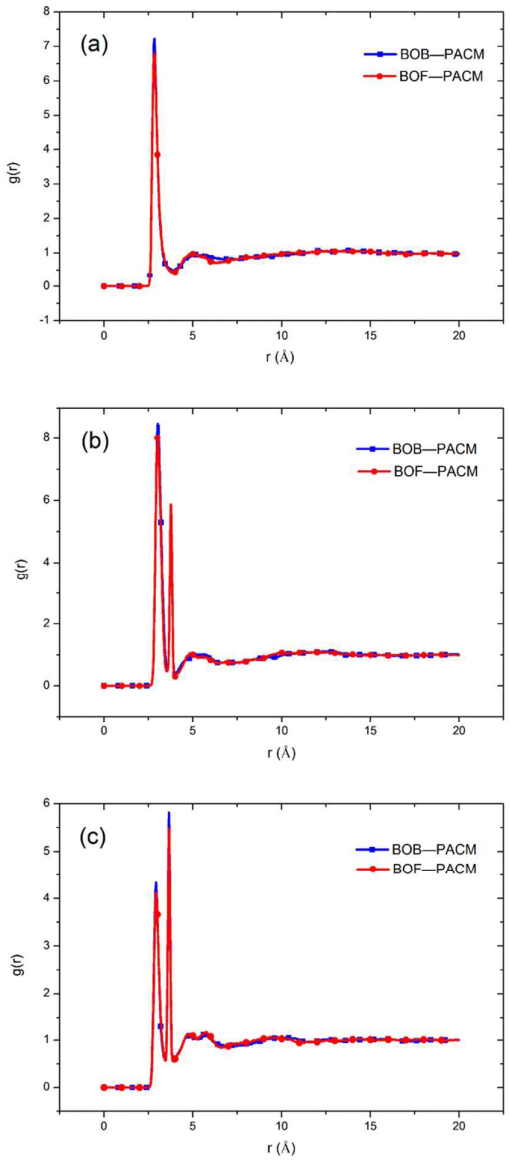

Figure 10. The RDFs for the three kinds of atom pairs: (a) hydroxy oxygen–ether oxygen, (b) hydroxy oxygen–nitrogen, and (c) hydroxy oxygen–hydroxy oxygen.

imply that the BOB–PACM system does not tend to generate more H–bonds. This result is inconsistent with that obtained in ref 37. But this is expected due to the only a little changes in the structure of BOF relative to that of BOB; in addition, the charge of the oxygen in the furan ring is lower than that in the ether because of the conjugated effect of the furan ring.

Free volumes

Free volume, proposed by Fox and Flory,[38] is a critically important concept in understanding atomic mobility in disordered structures like polymers. The free volume in the polymers can be determined by using the experimental methods, among which positron annihilation lifetime spectroscopy (PALS) [39,40] is the most common one. Molecular simulations provide an alternative method to measure the free volume of the materials.[41-45] Herein, we calculate the accessible free volume of the cross-linked systems utilizing the "Atom Volume & Surfaces" tool in the Material Studio software, which probes the polymer cell with a specified radius. According to Bondi,[45] the accessible free volume derived by the molecular simulation with a probe radius of about 0.4 Å is consistent with experimental ones. We adopt 0.4 Å as the probe radius to calculate these cross-linked systems. The free volumes of the two cross-linked systems as a function of temperature were plotted in Figure 11.

From Figure 11, we can see that at low temperature the free volume increase slowly, while at high temperature the free volume increase more sharply. According to Fox and Flory's theory,[46] the intersection of the bi-linear function is corresponding to the T_g, which is 354.65 K and 382.14 K for the BOB–PACM system and the BOF–PACM system, respectively. The results are close to those obtained from the volume–temperature data. Moreover, the free volume in the BOF–PACM cross-linked system is less than that in the BOB–PACM cross-linked system indicating higher packing efficiency of the BOF–PACM system.

Nonbond Energy

The simulated results of nonbond energy against the temperature were plotted in Figure 12. It can be seen that there is a break point in each of the curve, indicating the occurrence of glass transition. At both below and above T_g, nonbond energy increases almost linearly with increasing temperature with a break at T_g. This result is consistent with that of ref 19. Moreover, the nonbond energy in the BOB–PACM system is higher than that in the BOF–PACM system through all the temperatures. We conclude this leads to the difference of the free volume of the two cross-linked systems, i.e. the nonbond energy is one of the most important factors affecting the free volume in the polymer.

Further analysis was performed on the electrostatic energy and the vdW energy. Their values versus temperature were plotted in Figure 13. According to the monotonous increment of the vdW energy along with the temperature, we conclude the more negative vdW energy of the BOF–PACM system is mainly coming from the relatively closer distance between the atoms, i.e. the BOF–PACM system has higher packing efficiency than the BOF–PACM system. This deduction is consistent with that obtained from the free volume. It can be seen that the difference between the two systems in the vdW energy is more significant than that in the electrostatic energy through all the temperatures. Therefore, it can be concluded that compared with the electrostatic energy, the vdW energy plays a more important role in determining the difference of the thermomechanical properties between the two systems.

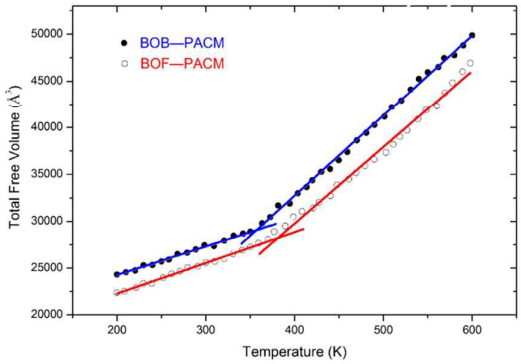

Figure 11. The free volume versus temperature of the two cross-linked systems: (a) BOB–PACM (b) BOF–PACM.

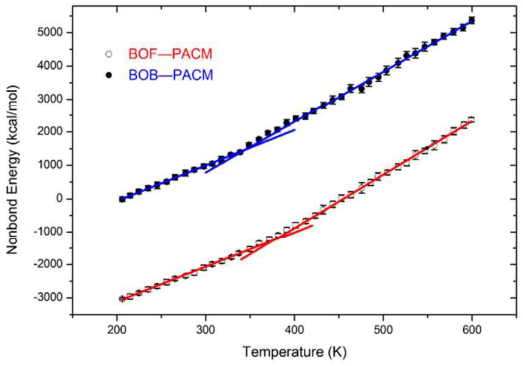

Figure 12. The nonbond energy–temperature relationships of BOB–PACM and BOF–PACM.

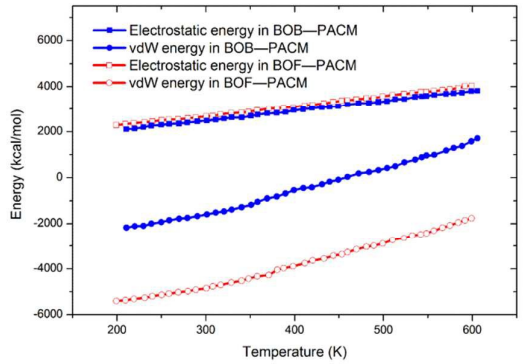

Figure 13. The electrostatic and van der Waals energy in BOB–PACM and BOF–PACM as a function of temperature.

Mobility of the Polymer Chains

The mobility of the polymer chains was characterized by calculating the mean square displacement (MSD) of certain groups of atoms. The MSD is calculated as follows:

$$\mathrm{MSD}=\frac{1}{3N}\sum_{i=0}^{N-1}\left\langle\left|\vec{R}_i(t)-\vec{R}_i(0)\right|^2\right\rangle \quad (6)$$

where *R* and *N* is the spatial position and the total number of the particles studied, respectively, *t* is the corresponding time, and the angle brackets represent an average over all choices of time origin.

In this work, we pay special attention to the aromatic rings in the epoxy monomers and the dicyclohexylmethane in the cross-linker PACM. Figure 14 plots the MSD versus time curves of these sets of atoms in the BOB–PACM and BOF–PACM systems for the first 100 ps, at 200 K. It is obvious that the MSD values in the BOB–PACM are higher than those in the BOF–PACM system, which indicates that the mobility of the polymer chains in the BOB–PACM system is stronger than that in the BOF–PACM system. The weaker mobility of the polymer chains in the BOF–PACM system can be interpreted by the steric restriction arising from the vdW energy. It is important to emphasize here that besides the aromatic rings in the epoxy monomers, the dicyclohexylmethane in the cross-linker PACM in the BOF–PACM system also has more mobility than that in the BOB–PACM system. This highlights the importance of the intermolecular interactions rather than the symmetry of the aromatic rings on the properties of these cross-linked epoxy systems which will only affect the mobility of the aromatic structures. So the BOF–PACM system shows higher chain packing efficiency than the BOB–PACM system, and this leads to lower mobility of the polymer chains.

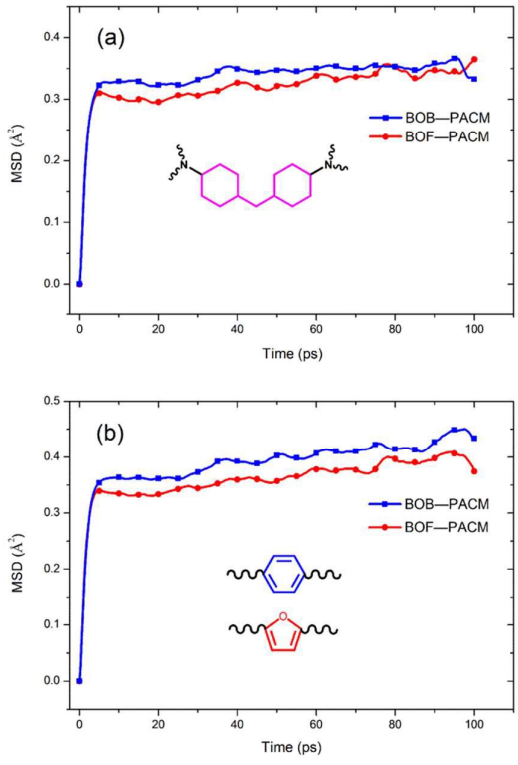

Figure 14. The MSD curves of (a) dicyclohexylmethane in PACM and (b) aromatic rings in the epoxy monomers for BOF–PACM and BOF–PACM.

Conclusions

In this paper, two well-relaxed cross-linked epoxy systems, BOB–PACM and BOF–PACM, were carefully constructed with the cross-linking degrees both being exactly 90% by using a stepwise cross-linking algorithm. Polymer Consistent Force-Field was used to describe atomic interactions.

These two systems have very similar structures with the only change from benzene ring to furan ring in the epoxy monomers. By comparing the two systems, we try to explore the influence of the detailed chemical structure of epoxy monomer on the thermomechanical properties, especially the glassy Young's modulus, of the cross-linked epoxy systems.

A wide range of thermomechanical properties such as glass transition temperatures, coefficient of thermal expansions, glassy Young's moduli, Poisson's ratios of the two systems were characterized and then compared with the available experimental data. Good agreements were obtained, which proves the validity of the models established in this work.

Glassy Young's moduli were predicted from the stress–strain curves. Same to the experimental data, glassy elastic modulus of the BOF–PACM system is higher than that of the BOB–PACM system. The effects of epoxy monomer structure on the glassy Young's modulus were evaluated by calculating the H–bonds and nonbond energy, comparing the difference of the free volume, and analyzing the mobility of the polymer chains. Different from the results in ref 37, the H–bonds in the BOF–PACM system described by the RDFs of specific atoms are almost the same as those in the BOB–PACM system. However, compared with the BOB–PACM system, the BOF–PACM system has less free volume and larger vdW energy through all the temperatures from 200 K to 600 K, which indicates higher packing efficiency of the BOF–PACM system. We conclude these are the reasons why the BOF–PACM system has weaker mobility of the polymer chains, which is illustrated by the lower MSD values of both the aromatic rings in the epoxy monomers and the dicyclohexylmethane in the cross-linker in the BOF–PACM system. To sum up, it is the high packing density arising from the strong polarity that leads to weak mobility of the polymer chains because of the steric restriction, and finally contributes to high glassy Young's modulus.

Through the analysis above, we confirm that MD simulations provide a useful tool to construct the highly cross-linked systems, predict their thermomechanical properties, and study the structure–property relationships of the cross-linked thermosetting materials. This is our first step to analyze effects of the monomer structures on the thermomechanical properties, more molecular simulations will be performed to further analyze the structure–property relationships of the cross-linked epoxy networks.

Acknowledgements

The authors acknowledge the financial support from the National Natural Science Foundation of China under Grant No. 21476013.

Notes and references

1 A. Siegmann, A. Buchman and S. Kenig, *Polymer Engineering & Science*, 1981, **21**, 997-1002.
2 J. Lange, S. Toll, J.-A. E. Månson and A. Hult, *Polymer*, 1997, **38**, 809-815.
3 A. A. Roche and J. Guillemenet, *Thin Solid Films*, 1999, **342**, 52-60.
4 S. L. Case, E. P. O'Brien and T. C. Ward, *Polymer*, 2005, **46**, 10831-10840.
5 J. Lange, S. Toll, J.-A. E. Månson and A. Hult, *Polymer*, 1995, **36**, 3135-3141.
6 V. B. Gupta and C. Brahatheeswaran, *Polymer*, 1991, **32**, 1875-1884.
7 X. Wang, *Journal of Applied Polymer Science*, 1997, **64**, 69-75.
8 R. J. Varley, J. H. Hodgkin and G. P. Simon, *Journal of Applied Polymer Science*, 2000, **77**, 237-248.
9 X. Wang and V. J. Foltz, *Polymer*, 2006, **47**, 5090-5096.
10 J. Moosburger-Will, M. Greisel, M. G. R. Sause, R. Horny and S. Horn, *Journal of Applied Polymer Science*, 2013, **130**, 4338-4346.
11 I. Yarovsky and E. Evans, *Polymer*, 2002, **43**, 963-969.
12 C. Wu and W. Xu, *Polymer*, 2006, **47**, 6004-6009.
13 V. Varshney, S. S. Patnaik, A. K. Roy and B. L. Farmer, *Macromolecules*, 2008, **41**, 6837-6842.
14 J. L. Tack and D. M. Ford, *Journal of Molecular Graphics and Modelling*, 2008, **26**, 1269-1275.
15 C. Li and A. Strachan, *Polymer*, 2010, **51**, 6058-6070.
16 C. Li and A. Strachan, *Polymer*, 2011, **52**, 2920-2928.
17 N. J. Soni, P.-H. Lin and R. Khare, *Polymer*, 2012, **53**, 1015-1019.
18 C. Li, G. A. Medvedev, E.-W. Lee, J. Kim, J. M. Caruthers and A. Strachan, *Polymer*, 2012, **53**, 4222-4230.
19 S. Yang and J. Qu, *Polymer*, 2012, **53**, 4806-4817.
20 Q. Yang, X. Yang, X. Li, L. Shi and G. Sui, *RSC Advances*, 2013, **3**, 7452-7459.
21 G. M. Odegard, B. D. Jensen, S. Gowtham, J. Wu, J. He and Z. Zhang, *Chemical Physics Letters*, 2014, **591**, 175-178.
22 T. W. Sirk, M. Karim, K. S. Khare, J. L. Lenhart, J. W. Andzelm and R. Khare, *Polymer*, 2015, **58**, 199-208.
23 H. Sun, *Journal of Computational Chemistry*, 1994, **15**, 752-768.
24 H. Sun, *Macromolecules*, 1995, **28**, 701-712.
25 L.-h. Tam and D. Lau, *RSC Advances*, 2014, **4**, 33074-33081.
26 H. B. Fan and M. M. F. Yuen, *Polymer*, 2007, **48**, 2174-2178.
27 Materials Studio, Accelrys Software Inc.
28 D. N. Theodorou and U. W. Suter, *Macromolecules*, 1985, **18**, 1467-1478.
29 D. N. Theodorou and U. W. Suter, *Macromolecules*, 1986, **19**, 139-154.
30 T. C. Clancy, S. J. V. Frankland, J. A. Hinkley and T. S. Gates, *Polymer*, 2009, **50**, 2736-2742.
31 V. Varshney, S. S. Patnaik, A. K. Roy and B. L. Farmer, *Polymer*, 2009, **50**, 3378-3385.
32 T. Oie, G. M. Maggiora, R. E. Christoffersen and D. J. Duchamp, *International Journal of Quantum Chemistry*, 1981, **20**, 1-47.
33 F. F. de Nograro, R. Llano-Ponte and I. Mondragon, *Polymer*, 1996, **37**, 1589-1600.
34 M. L. Williams, R. F. Landel and J. D. Ferry, *Journal of the American Chemical Society*, 1955, **77**, 3701-3707.
35 A. Bandyopadhyay, P. K. Valavala, T. C. Clancy, K. E. Wise and G. M. Odegard, *Polymer*, 2011, **52**, 2445-2452.
36 S. Wang, Z. Liang, P. Gonnet, Y. H. Liao, B. Wang and C. Zhang, *Advanced Functional Materials*, 2007, **17**, 87-92.
37 F. Hu, J. J. La Scala, J. M. Sadler and G. R. Palmese, *Macromolecules*, 2014, **47**, 3332-3342.
38 T. G. Fox and P. J. Flory, *Journal of Applied Physics*, 1950, **21**, 581-591.
39 S. Goyanes, W. Salgueiro, A. Somoza, J. A. Ramos and I. Mondragon, *Polymer*, 2004, **45**, 6691-6697.
40 M. Blanco, J. A. Ramos, S. Goyanes, G. Rubiolo, W. Salgueiro, A. Somoza and I. Mondragon, *Journal of Polymer Science Part B: Polymer Physics*, 2009, **47**, 1240-1252.
41 S. Jiang, K. E. Jelfs, D. Holden, T. Hasell, S. Y. Chong, M. Haranczyk, A. Trewin and A. I. Cooper, *Journal of the American Chemical Society*, 2013, **135**, 17818-17830.
42 X.-Y. Wang, F. T. Willmore, R. D. Raharjo, X. Wang, B. D. Freeman, A. J. Hill and I. C. Sanchez, *The Journal of Physical Chemistry B*, 2006, **110**, 16685-16693.
43 P. M. Budd, N. B. McKeown and D. Fritsch, *Journal of Materials Chemistry*, 2005, **15**, 1977-1986.
44 X.-Y. Wang, K. M. Lee, Y. Lu, M. T. Stone, I. C. Sanchez and B. D. Freeman, *Polymer*, 2004, **45**, 3907-3912.
45 D. Hofmann, M. Heuchel, Y. Yampolskii, V. Khotimskii and V. Shantarovich, *Macromolecules*, 2002, **35**, 2129-2140.
46 T. G. Fox and S. Loshaek, *Journal of Polymer Science*, 1955, **15**, 371-390.

For Table of Contents

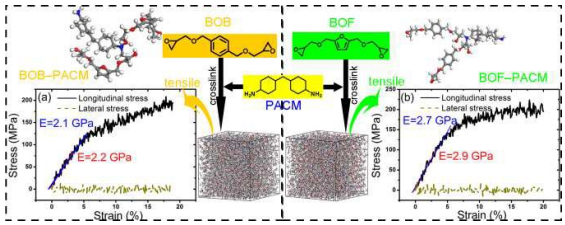

Higher van der Waals interactions arising from furan ring leads to improved thermomechanical properties of cross-linked epoxy network.